



## <sup>18</sup>F-Labeled FECNT: A Selective Radioligand for PET Imaging of Brain Dopamine Transporters

Mark M. Goodman,<sup>1</sup> Clinton D. Kilts,<sup>2</sup> Robert Keil,<sup>1</sup> Bing Shi,<sup>1</sup>  
Laurent Martarello,<sup>1</sup> Dongxia Xing,<sup>1</sup> John Votaw,<sup>1</sup> Timothy D. Ely,<sup>2</sup> Philip Lambert,<sup>2</sup>  
Michael J. Owens,<sup>2</sup> Vernon M. Camp,<sup>1</sup> Eugene Malveaux<sup>1</sup> and John M. Hoffman<sup>3</sup>

DEPARTMENTS OF <sup>1</sup>RADIOLOGY, <sup>2</sup>PSYCHIATRY AND BEHAVIOR SCIENCES, AND <sup>3</sup>NEUROLOGY, EMORY CENTER FOR POSITRON EMISSION TOMOGRAPHY, EMORY UNIVERSITY, ATLANTA, GEORGIA, USA

**ABSTRACT.** Fluorine-18 labeled 2 $\beta$ -carbomethoxy-3 $\beta$ -(4-chlorophenyl)-8-(2-fluoroethyl)nortropine (FECNT) was synthesized in the development of a dopamine transporter (DAT) imaging ligand for positron emission tomography (PET). The methods of radiolabeling and ligand synthesis of FECNT, and the results of the *in vitro* characterization and *in vivo* tissue distribution in rats and *in vivo* PET imaging in rhesus monkeys of [<sup>18</sup>F]FECNT are described. Fluorine-18 was introduced into 2 $\beta$ -carbomethoxy-3 $\beta$ -(4-chlorophenyl)-8-(2-fluoroethyl)nortropine (4) by preparation of 1-[<sup>18</sup>F]fluoro-2-tosyloxyethane (2) followed by alkylation of 2 $\beta$ -carbomethoxy-3 $\beta$ -(4-chlorophenyl)nortropine (3) in 21% radiochemical yield (decay corrected to end of bombardment [EOB]). Competition binding in cells stably expressing the transfected human DAT serotonin transporter (SERT) and norepinephrine transporter (NET) labeled by [<sup>3</sup>H]WIN 35428, [<sup>3</sup>H]citalopram, and [<sup>3</sup>H]nisoxetine, respectively, indicated the following order of DAT affinity: GBR 12909 > CIT >> 2 $\beta$ -carbomethoxy-3 $\beta$ -(4-chlorophenyl)-8-(3-fluoropropyl)nortropine (FPCT) > FECNT. The affinity of FECNT for SERT and NET was 25- and 156-fold lower, respectively, than for DAT. Blocking studies were performed in rats with a series of transporter-specific agents and demonstrated that the brain uptake of [<sup>18</sup>F]FECNT was selective and specific for DAT-rich regions. PET brain imaging studies in monkeys demonstrated high [<sup>18</sup>F]FECNT uptake in the caudate and putamen that resulted in caudate-to-cerebellum and putamen-to-cerebellum ratios of 10.5 at 60 min. [<sup>18</sup>F]FECNT uptake in the caudate/putamen peaked in less than 75 min and exhibited higher caudate- and putamen-to-cerebellum ratios at transient equilibrium than reported for <sup>11</sup>C-WIN 35,428, [<sup>11</sup>C]CIT/RTI-55, or [<sup>18</sup>F]  $\beta$ -CIT-FP. Analysis of monkey arterial plasma samples using high performance liquid chromatography determined that there was no detectable formation of lipophilic radiolabeled metabolites capable of entering the brain. In equilibrium displacement experiments with CIT in rhesus monkeys, radioactivity in the putamen was displaced with an average half-time of 10.2 min. These results indicate that [<sup>18</sup>F]FECNT is a radioligand that is superior to <sup>11</sup>C-WIN 35,428, [<sup>11</sup>C]CIT/RTI-55, [<sup>18</sup>F] $\beta$ -CIT-FP, and [<sup>18</sup>F]FPCT for mapping brain DAT in humans using PET. NUCL MED BIOL 27;1:1–12, 2000. © 2000 Elsevier Science Inc. All rights reserved.

**KEY WORDS.** Fluorine-18 FECNT, Dopamine transporter, Fluorotropane, Cocaine

### INTRODUCTION

The brain dopamine transporter (DAT) is critical to dopamine neurotransmission and the psychostimulant effects of cocaine (6, 12, 27) and is decreased by Parkinson's disease (3, 17, 26). A major recent effort has focused on the development of radiolabeled DAT ligands to study the physiology, pharmacology, and pathophysiology of the brain DAT using positron emission tomography (PET). Initial attempts focused on nortropans labeled with carbon-11 or fluorine-18. PET imaging studies of DAT labeling with [<sup>11</sup>C]nomifensine in nonhuman and human primates have been reported (1). [<sup>11</sup>C]Nomifensine rapidly entered the brain but exhibited a low DAT selectivity that resulted in relatively low striatum-to-cerebellum binding ratios (1.53 at 50 min). A fluorine-18 analogue of a class of DAT selective aryl 1,4-dialkylpiperazines has also been developed for PET studies (18–20). Imaging

studies with [<sup>18</sup>F]GBR 13119 in nonhuman primates also indicated low DAT selectivity and resulted in low striatum-to-cerebellum ratios (1.51 at 50 min) comparable to those of [<sup>11</sup>C]nomifensine.

The tropane (-)-cocaine has been labeled with <sup>11</sup>C (10, 21) and used to examine brain DAT distribution in nonhuman and human primates. Several shortcomings of this product as a DAT radioligand are its nonselectivity, low binding affinity and rapid metabolism, which result in rapid binding site dissociation ( $t_{1/2}$  = 25 min), and its low target (striatum) to nontarget (cerebellum) binding ratios (e.g., 2.0). Dynamic PET imaging studies in baboons of brain DAT binding by the low affinity tropane [O-<sup>11</sup>C-methyl]d-threo-methylphenidate ([<sup>11</sup>C]d-threo-MP) has recently been reported (9). Serial PET images demonstrated that [<sup>11</sup>C]d-threo-MP accumulates in the DAT-rich striatum, with peak striatal uptake (0.05 %dose/g) occurring rapidly within 5–15 min postinjection. Moreover, [<sup>11</sup>C]d-threo-MP exhibited a low striatum-to-cerebellum ratio of 2.4:1 at 75 min postinjection.

A number of higher affinity DAT ligands, in which the 3 $\beta$ -(benzoyl) group of (-)-cocaine was replaced by 3 $\beta$ -(4-substituted-phenyl) groups, have been radiolabeled with carbon-11 for *in vivo* PET studies of the striatal DAT in nonhuman and human primates.

Address correspondence to: Mark M. Goodman, Ph.D., Department of Radiology, Emory University, 1364 Clifton Road, NE, Atlanta, GA 30322, USA; e-mail: mgoodma@emory.edu.

Received 12 September 1998.

Accepted 27 November 1998.

This group of DAT PET imaging agents includes [ $^{11}\text{C}$ ]2 $\beta$ -carbomethoxy-3 $\beta$ -(4-fluorophenyl)tropane ([ $^{11}\text{C}$ ]WIN 35,428) (8, 11, 24) and [ $^{11}\text{C}$ ]2 $\beta$ -carbomethoxy-3 $\beta$ -(4-iodophenyl)tropane ([ $^{11}\text{C}$ ]CIT/RTI-55) (25) and exhibits increased striatal uptake with low nonspecific binding relative to earlier agents. Replacement of the methyl group at the 8-position in CIT by either a 3-fluoropropyl group or a 2-fluoroethyl group yielded the [ $^{11}\text{C}$ ]labeled DAT ligands N-3-fluoropropyl-2 $\beta$ -carbomethoxy-3 $\beta$ -(4-iodophenyl)nortropane (O-methyl-[ $^{11}\text{C}$ ]FP-CIT) (22) and N-2-fluoroethyl-2 $\beta$ -carbomethoxy-3 $\beta$ -(4-iodophenyl)nortropane ([ $^{11}\text{C}$ ] $\beta$ -CIT-FE) (16), respectively. Radiosynthesis of fluorine-18 labeled FP-CIT has recently been reported (7) though in only a 1% radiochemical yield. Replacement of the 2 $\beta$ -carbomethoxy group in 2 $\beta$ -carbomethoxy-3 $\beta$ -(4-chlorophenyl)tropane by a 2 $\beta$ -carbo-2'-fluoroethoxy group yielded the DAT PET ligand FECNT radiolabeled with fluorine-18 (28).

Recently, we reported the synthesis of high specific activity (2 Ci/ $\mu\text{mole}$ ) fluorine-18 labeled 2 $\beta$ -carbomethoxy-3 $\beta$ -(4-chlorophenyl)-8-(3-fluoropropyl)nortropane (FPCT) as a new DAT PET imaging agent (15). PET imaging studies in rhesus monkeys with [ $^{18}\text{F}$ ]FPCT showed high radioligand uptake and retention in the putamen and caudate nucleus, brain regions that are rich in DAT, with low nonspecific binding in the DAT poor cerebellum and cerebral cortex. An undesired property accompanying DAT binding by [ $^{18}\text{F}$ ]FPCT, as well as by [ $^{11}\text{C}$ ]WIN 35,428 and [ $^{11}\text{C}$ ]CIT/RTI-55, is the need for a prolonged (>2 h) period required to reach binding equilibrium with the DAT. Unlike the parent, [ $^{11}\text{C}$ ]CIT/RTI-55, O-methyl-[ $^{11}\text{C}$ ]FP-CIT, and [ $^{11}\text{C}$ ] $\beta$ -CIT-FE DAT binding have been reported to reach equilibrium (16, 22). PET imaging studies with [ $^{11}\text{C}$ ] $\beta$ -CIT-FE in nonhuman primates exhibited high (9:1) caudate-to-cerebellum values at the time of transient equilibrium, which occurred 60 min postinjection. PET imaging with [ $^{18}\text{F}$ ]FP-CIT in humans and nonhuman primates also has been reported (7, 23). [ $^{18}\text{F}$ ]FP-CIT in nonhuman primates exhibited high 5:1 caudate-to-cerebellum values at the time of transient equilibrium, which occurred 60–100 min postinjection.

For PET studies, fluorine-18 offers significant advantages in comparison to the short 20 min half-life of carbon-11. The 110 min half-life of fluorine-18 allows sufficient time ( $3 \times 110$  min) for isotope incorporation into the tracer molecule and its purification to a final product suitable for human administration and permits the preparation of multidose batches for distribution by a cyclotron based radiopharmacy. Fluorine-18 is also the lowest energy positron emitter (0.635 MeV, 2.4 mm positron range) and affords the highest PET resolution images. Thus, the development of DAT ligands labeled with fluorine-18 that achieve high (>10) caudate/putamen-to-cerebellum ratios and exhibit more favorable kinetics (e.g., peak caudate/putamen-to-cerebellum ratios achieved in less than 2 h) would be ideal candidates for quantitative *in vivo* mapping of brain DAT sites by PET.

During attempts (14, 15) to develop a fluorine-18 labeled PET probe that exhibits high brain uptake and high selectivity and affinity for the DAT, we identified an alternative N-substituted fluoroalkyl derivative, 2 $\beta$ -carbomethoxy-3 $\beta$ -(4-chlorophenyl)-8-(2-fluoroethyl)nortropane (FECNT) with lower nanomolar affinity than FPCT for DAT (15). A potential advantage of employing a lower affinity selective DAT radioligand such as [ $^{18}\text{F}$ ]FECNT is that the radioligand may have a higher rate of dissociation from the DAT binding site, attain binding equilibrium more rapidly, and thus allow measurement of the DAT density from a single-frame image, avoiding the need for more complicated multicompartment kinetic models. In this article, we report the *in vitro* characterization

of FECNT as a DAT ligand, the radiosynthesis of high specific activity [ $^{18}\text{F}$ ]FECNT in 20% (corrected for decay at end of bombardment [EOB]) radiochemical yield, a comparison with [ $^{18}\text{F}$ ]FPCT of the kinetics of regional brain radioactivity using PET, and the *in vivo* displacement of brain  $^{18}\text{F}$ -FECNT binding by CIT in rhesus monkeys.

## EXPERIMENTAL

All animal experiments were carried out according to protocols approved by the Institutional University Animal Care Committee and Radiation Safety Committees of Emory University.

### FECNT Radiolabeling

Approximately 280  $\mu\text{L}$  of 95% enriched [ $^{18}\text{O}$ ]H $_2$ O containing 283 mCi NCA [ $^{18}\text{F}$ ]fluoride (Siemens RDS 112, Knoxville, TN USA) was added to a Wheaton 5 mL micro-vial (Millville, NJ USA) containing 1 mL of a solution of 10 mg Kryptofix (K-222) (Aldrich Chemical, Milwaukee, WI USA) and 1 mg potassium carbonate in 0.05 mL water and 0.95 mL CH $_3$ CN. The solution was heated at 116°C for 3.5 min after which three additional portions of 1 mL CH $_3$ CN were added and evaporated to dry the fluoride. The vial was cooled to room temperature and 1.5 mg of 1,2-ditosyloxyethane dissolved in 1.0 mL CH $_3$ CN was added. The solution was heated to 80°C for 10 min, cooled to room temperature, diluted with 5 mL of ether, and passed through a Waters classic SiO $_2$  Sep-pak<sup>®</sup> (Milford, MA USA) into a 10 mL maxi-vial attached to a 50 mL round bottomed flask. The sep-pak was rinsed with 5 mL of Et $_2$ O, which was added to the maxi-vial, bringing the total volume to 10 mL. The resulting ethereal solution was evaporated *in vacuo* and transferred to a 5 mL vial to yield 152 mCi of 1-[ $^{18}\text{F}$ ]fluoro-2-tosyloxyethane (2) (5). Four milligrams of 2 $\beta$ -carbomethoxy-3 $\beta$ -(4-chlorophenyl)nortropane (3) dissolved in 0.5 mL DMF, was added to the 1-[ $^{18}\text{F}$ ]fluoro-2-tosyloxyethane and the sealed vial was heated at 135°C for 0.75 h, at which time the solution was cooled to ambient temperature. The solution was diluted to 0.5 mL with 3/1/0.1% methanol/water/triethylamine and injected onto a reverse phase prep high pressure liquid chromatography (HPLC) column, (Waters, 25 mm  $\times$  100 mm, flow rate 6 mL/min). The fraction eluting at 20 min contained 26.5 mCi of the desired product, in a synthesis/purification time of 122 min. Thin layer chromatography (TLC) analysis using a radioactivity detector (SiO $_2$  90:10 CH $_2$ Cl $_2$ : CH $_3$ OH, R $_f$  = 0.6) and HPLC analysis (Waters C $_{18}$ , 8 mm  $\times$  200 mm Novapak, 3/1/0.25% methanol/water/triethylamine, flow rate 1 mL/min, rt = 4.3 min) using an ultraviolet (UV) detector and a radioactivity detector showed these fractions to have a chemical and radiochemical purity of greater than 99%. Fractions containing the greatest radioactivity were concentrated *in vacuo*, dissolved in sterile saline with 10% ethanol, and filtered through a Millipore 0.2  $\mu$  filter for *in vivo* studies.

### In Vitro Binding Experiments

**HOMOGENATES.** Monoamine transporter binding assays used cell membranes from either a dog kidney (MDCK) cell line stably transfected with the human DAT cDNA (gift of Dr. Gary Rudnick, Yale University) or a human embryonic kidney cell line (HEK-293) stably transfected with either the human serotonin (hSERT) or human norepinephrine transporter (hNET) cDNA (gift of Dr. Randy Blakely, Vanderbilt University). Cells were grown to con-

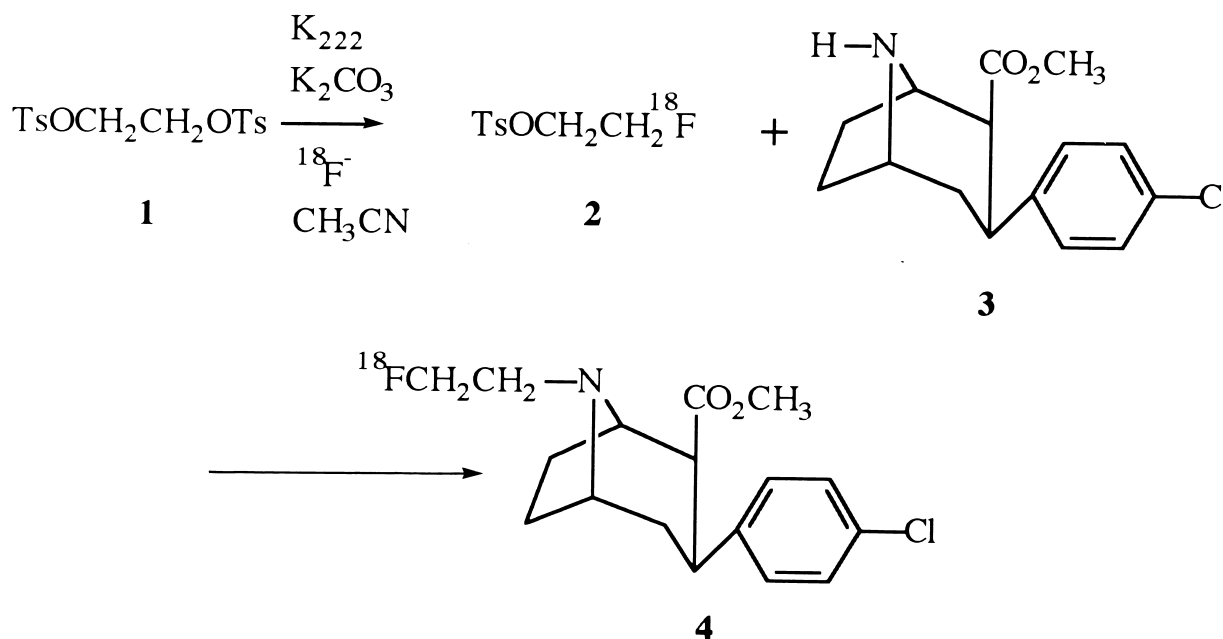


**FIG. 1. Synthesis of fluorine-18 labeled 2β-carbomethoxy-3β-(4-chlorophenyl)-8-(2-fluoroethyl)nortropene ([<sup>18</sup>F]FECNT)**

fluency in DMEM containing 10% fetal bovine serum and geneticin sulfate and harvested using 37°C phosphate-buffered saline (PBS, pH 7.4) containing ethylenediaminetetraacetic acid (EDTA). Following centrifugation (2,000 × g, 10 min), the supernatants were decanted and the pellets homogenized with a Polytron PT3000 (Brinkman, Littau, Switzerland; 11,000 rpm for 12 s) in 30 volumes of PBS and centrifuged at 43,000 × g for 10 min. The supernatants were decanted and the resulting pellets stored at −70°C until assayed.

Binding assays were carried out in 12 × 75 mm polystyrene tubes in a 1,000 μL volume consisting of 700 μL of assay buffer, 100/μL of competing ligand, 100 μL of <sup>3</sup>H ligand, and 100 μL of membrane suspension. Prior to each assay, the cell lines were characterized to determine a membrane concentration that yielded optimal binding. Membrane suspensions were prepared by resuspending the pellet in 5 mL of assay buffer and centrifuging (400 × g, 10 min). The supernatant was decanted and the resulting pellet resuspended in assay buffer and briefly homogenized using a Polytron PT3000. Competing ligands were assayed in triplicate at each of nine concentrations (10<sup>−13</sup> to 10<sup>−6</sup> M). The ligands were first dissolved in absolute ethanol at 10<sup>−3</sup> M then serially diluted in 2.5 mM HCl. A monoamine transporter-selective ligand of known binding affinity (DAT, GBR 12909; hSERT, fluvoxamine; hNET, desipramine) was included as a reference in each assay. For DAT binding, the assay buffer was 0.03 M phosphate buffer (pH 7.4) containing 0.32 M sucrose, the radioligand was [<sup>3</sup>H]WIN 35,428 (Dupont NEN, Boston MA USA; 84.5 Ci/mmol, 2.0 nM final concentration), and the equilibrium incubation time was 2 h at 4°C. For hSERT binding, the assay buffer was 50 mM Tris, 120 mM NaCl, and 5 mM KCl (pH 7.9), the radioligand was [<sup>3</sup>H]citalopram (Dupont NEN; 85.7 Ci/mmol, 0.5 nM final concentration), and the equilibrium incubation time was 1 h at 22°C. For hNET binding, the assay buffer was 50 mM Tris, 300 mM NaCl, and 5 mM KCl (pH 7.4), the radioligand was [<sup>3</sup>H]nisoxetine (Dupont NEN; 85.9 Ci/mmol, 0.55 nM final concentration), and the incubation time was 4 h at 4°C. All assays were initiated by the addition of membrane suspension.

Incubations were terminated by the addition of 2 mL of 0.03 M phosphate buffer (pH 7.4, 4°C) and rapid vacuum filtration through GF/B filters (presoaked in phosphate buffer containing 0.3% polyethyleneimine) with four washes (5 mL) of 0.03 M phosphate buffer (pH 7.4, 4°C). The filters were then dried and placed in scintillation vials to which 6 mL of scintillation cocktail (Aquasol-2, Packard, Meriden, CT USA) was added. The vials were shaken and radioactivity determined in a liquid scintillation counter at 66% efficiency. The data from the competition binding curves were analyzed and K<sub>i</sub> values generated using GraphPad Prism software (GraphPad Software, San Diego, CA USA).

**IN VITRO AUTORADIOGRAPHY.** A cerebral hemisphere of a rhesus (macaca mulatta) monkey was sliced into coronal sections of 20 μm thickness using a cryostat and the sections mounted on glass slides, air dried, and stored at −20°C. Following desiccation under vacuum (20 h at 4°C), the tissue was fixed for 2 min in 0.1% paraformaldehyde at 4°C, washed twice (15 min) in 0.1 M phosphate buffer (pH 7.4, 22°C), and incubated in a solution of 1 nM [<sup>18</sup>F]FECNT (determined at the beginning of the experiment) in 0.1 M phosphate buffer for 30 min at 22°C. The slides were then washed twice (5 min in a 0.1 M phosphate buffer, dipped in deionized water, and dried under a stream of cold air). The slides and a set of standards were then apposed to BioMax film (Kodak) for 1 h and the autoradiograms developed. The standards were constructed by blotting known amounts (0.02–2.5 μCi) of [<sup>18</sup>F]FECNT onto circles (1 cm diameter) of filter paper. Digital images of the autoradiograms were collected using the MCID imaging software system (Imaging Research Ins., Toronto, Ontario, Canada) and optical density readings were automatically converted to activity per millimeter squared values based on the standard curve.

### In Vivo Blocking Experiments

Regional brain distribution after intravenous administration of [<sup>18</sup>F]FECNT was determined in dissected tissues from male Sprague-Dawley rats (250–300 g). The animals were allowed food and water

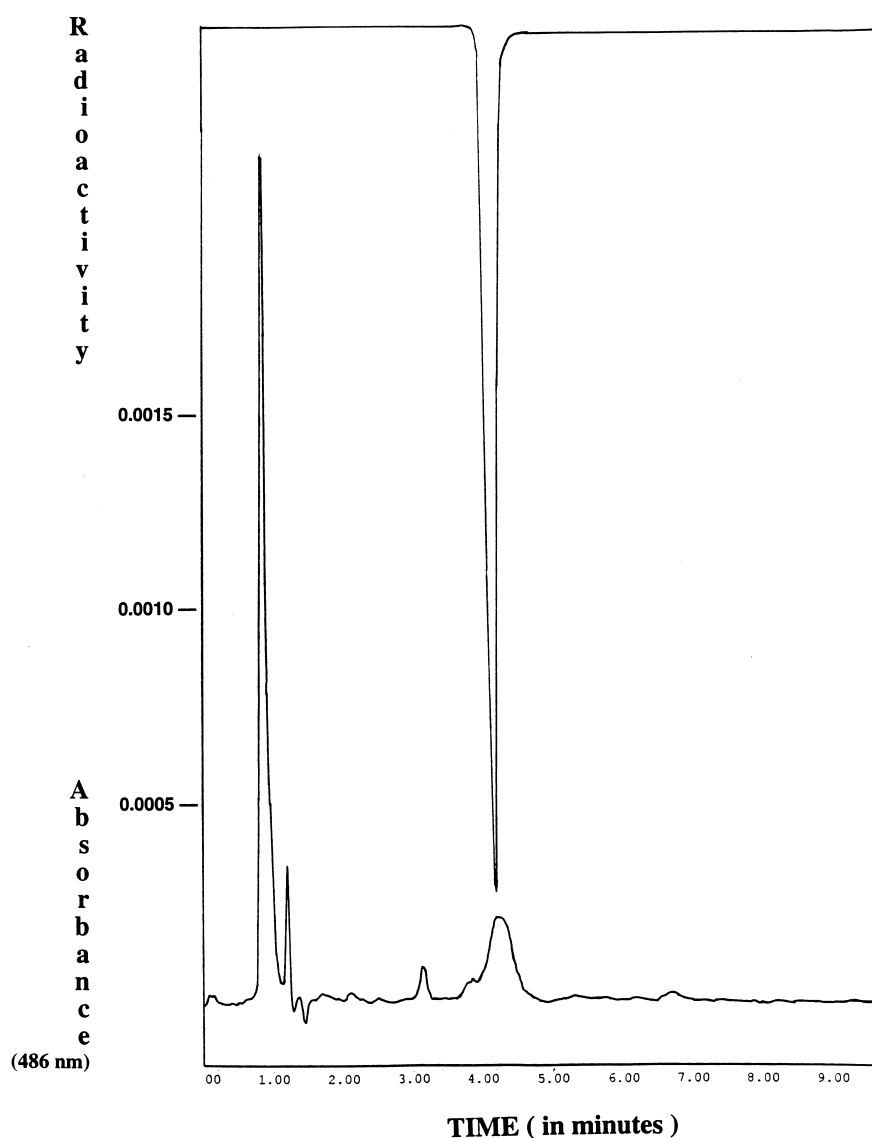


**FIG. 2.** Analytical high performance liquid chromatogram (radioactivity and ultraviolet versus time) of fluorine-18 labeled 2 $\beta$ -carbomethoxy-3 $\beta$ -(4-chlorophenyl)-8-(2-fluoroethyl)nortropine ( $[^{18}\text{F}]\text{FECNT}$ ) and  $[^{19}\text{F}]\text{FECNT}$  using a Waters  $\text{C}_{18}$  8 mm  $\times$  200 mm Novapak column.

ad libitum prior to the experiment. The rats were anesthetized by an intramuscular injection of 0.1 mL/100 g of a 50:50 mixture of ketamine (50 mg/mL) and xylazine (20 mg/mL).  $[^{18}\text{F}]\text{FECNT}$  (60  $\mu\text{Ci}$ ) in 0.2 mL of 10% ethanol in 0.9% NaCl was injected directly into the tail vein of the rats while under anesthesia. The animals were sacrificed 60 min postinjection with an intramuscular injection of 0.2 mL/kg of Euthansia-5 (324 mg/50 mL, sodium pentobarbital) under anesthesia. For the blocking experiments, one group was injected with GBR 12909 (5 mg/kg) directly into the tail vein 15 min prior to injection of  $[^{18}\text{F}]\text{FECNT}$ . Another group of rats was injected intravenously with paroxetine (5 mg/kg) 15 min prior to injection of  $[^{18}\text{F}]\text{FECNT}$ , a third group was injected intravenously with reboxetine (5 mg/kg) 15 min prior to injection of  $[^{18}\text{F}]\text{FECNT}$ , and a fourth group of rats was injected intravenously with  $[^{18}\text{F}]\text{FECNT}$  only as the control group. The striatum, cortex, prefrontal cortex, hypothalamus, and cerebellum were dissected and placed in tared test tubes. The test tubes were weighed, and radioactivity was determined with a Packard gamma automatic

counter (Model Cobra). The percent dose per gram was calculated by a comparison of decay corrected and background subtracted tissue counts with the counts of the dilution-corrected initial injected dose.

### Nonhuman Primate Imaging

Quantitative brain images were acquired in a 6-year-old rhesus monkey weighing 5.6 kg using a Siemens 951 31 slice PET imaging system. Images were reconstructed with a Shepp-Logan filter ( $0.35 \times$  Nyquist frequency) giving a resolution of 8 mm FWHM. The animal was initially anesthetized with intramuscular injection of Telazol<sup>®</sup> 3 mg/kg and maintained on a 1% isoflurane/5% oxygen mixture throughout the imaging procedure. The animal was intubated with assurance of adequate patency of the airway and was placed on a ventilator with arterial blood gases monitored throughout the study to assure physiologic levels of respiration. An arterial catheter was placed in a distal leg artery of the animal. The animal



**TABLE 1. Inhibition Constants (K<sub>i</sub>, nM) of Various Ligands for Monoamine Transporters**

Ligand	Human			Rat		
	DA*	5-HT†	NE‡	DA§	5-HT§	NE§
CIT	0.48	0.67	474			
FPCT	1.49	46.5	361	6.1	56.2	10,000
FECNT	1.53	39.1	240	7.95	21	10,000
GBR 12909	0.36					
Fluvoxamine		3.08				
Desipramine			3.02			

\* Competitive binding versus [N-methyl-<sup>3</sup>H]-WIN 35428 in murine kidney cells transfected with human dopamine transporter.

† Competitive binding versus [<sup>3</sup>H]citalopram in murine kidney cells transfected with human serotonin transporter.

‡ Competitive binding versus [N-methyl-<sup>3</sup>H]-nisoxetine in murine kidney cells transfected with human norepinephrine transporter.

§ 2–12 nM [N-methyl-<sup>3</sup>H]-WIN 35428, [<sup>3</sup>H]citalopram, or [<sup>3</sup>H]desmethylinpramine were incubated in the presence of 7–11 concentrations the indicated ligand and membranes prepared from rat striatum or cortex. The assays were performed by NOVASCREEEN in participation with the NIMH/NOVASCREEEN Psychotherapeutic Drug Discovery Development Program. DA = dopamine; HT = serotonin; NE = norepinephrine; FPCT = 2β-carboxymethoxy-3β-(4-chlorophenyl)-8-(3-fluoropropyl)nortropine.

was placed in the tomograph and the head was immobilized with a thermoplastic (Tru Scan, Annapolis, MD USA) face mask. A transmission scan was then obtained with a gallium source for attenuation correction of emission data. Either [<sup>18</sup>F]FECNT (5.88 mCi) or [<sup>18</sup>F]FPCT (3.13 mCi) was injected into an antecubital vein in a slow bolus infusion over 30 seconds. Arterial blood sampling (0.5 mL samples) was performed at approximately 10–12 s intervals with 12 samples obtained over the first 2 min. Arterial

samples were also obtained at 3, 4, 5, 7, 10, 20, 30, 60, 90, and 120 min after tracer injection. Kinetic emission data were acquired using either an 18-frame acquisition sequence that included six 30-s scans, four 3-min scans, five 10-min scans, and three 20-min scans, or a 20-frame acquisition sequence that included six 30-s scans, four 3-min scans, five 10-min scans, three 20-min scans, and two 30-min scans. Following [<sup>18</sup>F]FECNT and [<sup>18</sup>F]FPCT imaging, [<sup>15</sup>O]H<sub>2</sub>O (10 mCi) was injected and a 2-min scan was acquired and co-registered to the [<sup>18</sup>F]FECNT and [<sup>18</sup>F]FPCT images to identify regional brain structures. Bilateral regions of interest on the [<sup>15</sup>O]H<sub>2</sub>O co-registered [<sup>18</sup>F]FECNT and [<sup>18</sup>F]FPCT images were drawn manually for the caudate, putamen, thalamus, temporal cortex, and cerebellum. The data was displayed as both %dose/g and nCi/mL and normalized for the quantity of injected dose and the weight of the monkey.

### Pharmacologic Displacement in Nonhuman Primates

The validation of [<sup>18</sup>F]FECNT binding to DAT in the monkey putamen of two rhesus monkeys was assessed by its displacement by the potent DAT ligand RTI-55 (CIT). The dose of CIT for both studies was 0.9 μmole/kg administered 210 min following injection of [<sup>18</sup>F]FECNT (2.21 mCi). Quantitative brain images were acquired in the two rhesus monkeys using a Siemens 951 31 slice PET scanner with the collection of emission data initiated 90 min postinjection using a 14-frame acquisition sequence that included six 20-min scans and eight 5-min scans. Following the [<sup>18</sup>F]FECNT imaging protocol, a 15 min transmission scan was obtained with a gallium source for attenuation correction of emission data. Bilateral regions of interest were drawn for regional [<sup>18</sup>F]FECNT binding and displayed as nCi/mL and normalized for the quantity of injected dose and the weight of the monkey.

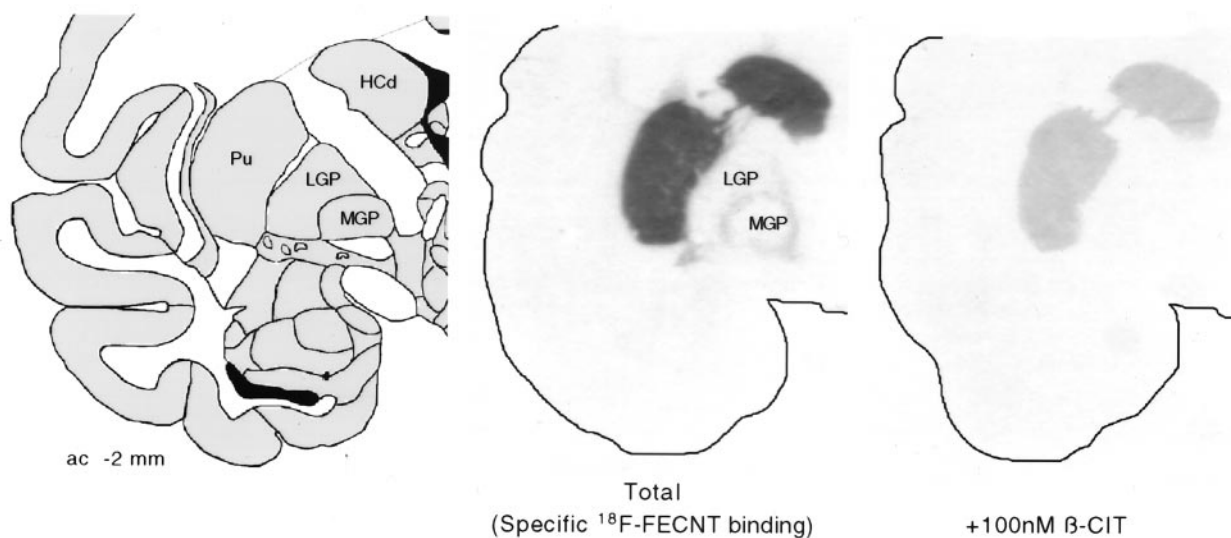


**FIG. 3.** Autoradiograms of fluorine-18 labeled 2β-carboxymethoxy-3β-(4-chlorophenyl)-8-(2-fluoroethyl)nortropine ([<sup>18</sup>F]FECNT) binding to coronal sections of the rhesus monkey brain. [<sup>18</sup>F]FECNT binding in the head of the caudate and putamen in the absence (total) and presence of 100 nM CIT is illustrated. The surface of the brain on the autoradiographic image was manually outlined and a reference drawing of the corresponding coronal plane (2 mm posterior to the anterior commissure) of the rhesus brain (from NeuroName and Template Atlas of the Primate Brain) are included to illustrate the localization of [<sup>18</sup>F]FECNT binding. Pu = putamen; HCd = head of the caudate nucleus; MGP = medial globus pallidus; LGP = lateral globus pallidus.

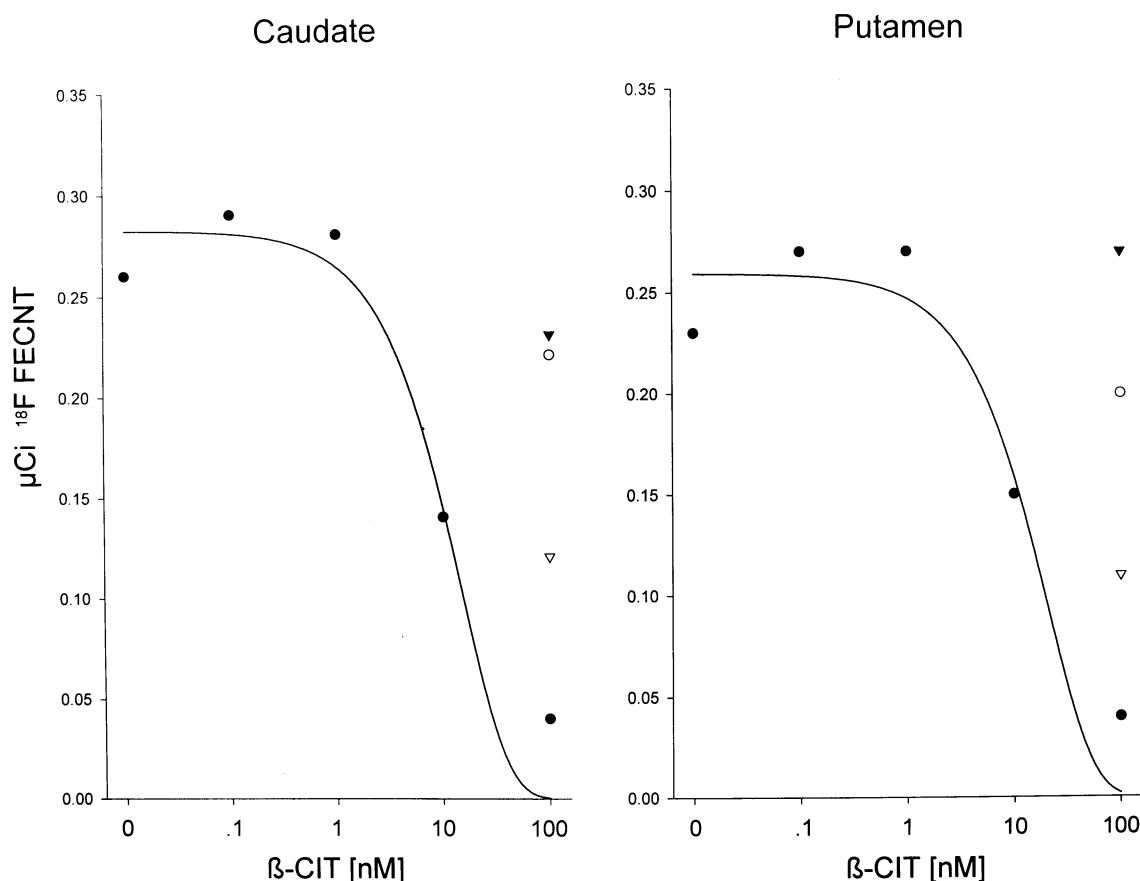


**FIG. 4.** Concentration-dependent displacement by CIT of the binding of fluorine-18 labeled 2 $\beta$ -carbomethoxy-3 $\beta$ -(4-chlorophenyl)-8-(2-fluoroethyl)nortropine ([ $^{18}\text{F}$ ]FECNT) to the head of the caudate and putamen of the rhesus monkey brain. The effect of 100 nM of paroxetine ( $\blacktriangle$ ), reboxetine (o), and GB 12909 ( $\Delta$ ) are included for comparison.

#### [ $^{18}\text{F}$ ]FECNT Metabolite Analysis (Monkey)

Arterial plasma analysis of [ $^{18}\text{F}$ ]FECNT metabolism was performed in four rhesus monkeys. Metabolite analysis was performed as described for [ $^{18}\text{F}$ ]FPCT (15). [ $^{18}\text{F}$ ]FECNT was injected as described above and arterial samples (5.0 mL) were collected at approximately 1, 2, 5, 15, 30, 60, and 120 min after tracer injection. Plasma was

prepared by centrifugation (3,000 g for 20 min) and nonpolar, brain permeable  $^{18}\text{F}$ -labeled metabolites extracted with ethyl ether ( $2 \times 1$  mL). The ethyl ether extracts of each plasma sample were evaporated to dryness under nitrogen at  $35^\circ\text{C}$ . The resulting residue was dissolved in 200  $\mu\text{L}$  of methanol/water/triethylamine (3/1/0.1%) and analyzed by HPLC with a UV detector (254 nm) and a flow-through

**TABLE 2.** Distribution of Radioactivity (%Injected Dose/g of Tissue) in Rats 60 min after Intravenous Administration of [ $^{18}\text{F}$ ]FECNT\*

Region	Study 1			Study 2	
	†No blocker	†GBR 12909	†Reboxetine	‡No blocker	‡,§Paroxetine
Striatum	2.24 (2.02–2.55)	1.21 (1.00–1.26)	2.69 (2.32–3.00)	0.95 (0.80–1.07)	1.03 (0.92–1.13)
Prefrontal cortex	1.17 (0.92–1.3)	0.94 (0.94–1.75)	1.06 (0.73–1.35)	0.31 (0.25–0.38)	0.29 (0.26–0.31)
Cortex	0.57 (0.39–0.89)	0.71 (0.43–1.08)	0.54 (0.51–1.16)	0.27 (0.23–0.29)	0.18 (0.17–0.20)
Hypothalamus	1.00 (0.72–1.25)	1.14 (1.02–1.26)	1.11 (0.76–1.36)	0.54 (0.36–0.67)	0.48 (0.45–0.51)
Cerebellum	0.28 (0.22–0.31)	0.33 (0.28–0.44)	0.26 (0.18–0.33)	0.22 (0.20–0.23)	0.14 (0.18–0.33)

\* Mean and range values for 4 male Sprague Dawley rats.

† Tissue studies performed with same batch of fluorine-18 labeled 2 $\beta$ -carbomethoxy-3 $\beta$ -(4-chlorophenyl)-8-(2-fluoroethyl)nortropine ([ $^{18}\text{F}$ ]FECNT).

‡ Tissue studies performed with same batch of [ $^{18}\text{F}$ ]FECNT.

§ Mean and range values for 3 male Sprague Dawley rats.

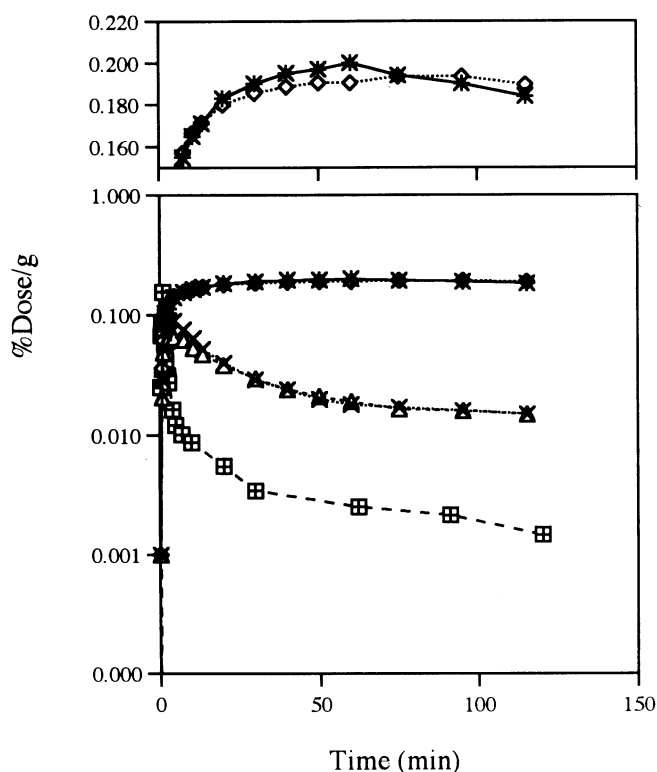


FIG. 5. Time-activity curves for average of left and right putamen (\*), left and right caudate (◇), cortex (Δ), cerebellum (X), and parent in plasma (□) for a rhesus monkey after receiving 5.88 mCi of fluorine-18 labeled 2β-carbomethoxy-3β-(4-chlorophenyl)-8-(2-fluoroethyl)nortropine ( $^{18}\text{F}$ ]FECNT). Serial images were acquired for a total time of 125 min (i.e., 18 scans).

radioactivity detector. Chromatographic separation used a Waters reverse phase  $\text{C}_{18}$  column (8 mm  $\times$  200 mm) and a mobile phase of methanol/water/triethylamine (3/1/0.1%) and flow rate of 1 mL/min. Eluate fractions (0.4 min) were collected and measured for radioactivity using an Packard Cobra automatic gamma-counter. Plasma protein bound radioactivity was measured (in duplicate) by ultra-filtration through membranes having a 30,000 molecular weight cut-off (Centrifree #4104, Amicon, W.R. Grace & Co., Danvers, MA USA) as described for  $^{123}\text{I}$ ]β-CIT (23).

#### $^{18}\text{F}$ ]FECNT Metabolite Analysis (Rat)

Male Sprague-Dawley rats weighing approximately 500 g were injected intravenously with 0.5 mL of 10% ethanol:saline (0.9%) containing 2.0 mCi of  $^{18}\text{F}$ ]FECNT. Groups (N = 2) of rats were euthanized as described above for the blocking studies at 2 and 60 min postinjection and brains were rapidly removed. The striatum was dissected and homogenized in a solution of 1 mg of FECNT tartrate salt in 1.0 mL of saline. The resulting homogenate was extracted with ethyl ether (2  $\times$  1.0 mL). The ethyl ether extracts were evaporated to dryness under nitrogen at 35°C. The resulting residue was dissolved in 300  $\mu\text{L}$  of methanol/water/triethylamine (3/1/0.1%) and HPLC eluates analyzed for mass (Waters 486 variable wave length absorbance detector) and radioactivity (Packard Cobra automatic gamma-counter). A similar method has been reported by Billings (4) for investigation of the metabolism of R(+)- $^{123}\text{I}$ ]TISCH in rat striatum.

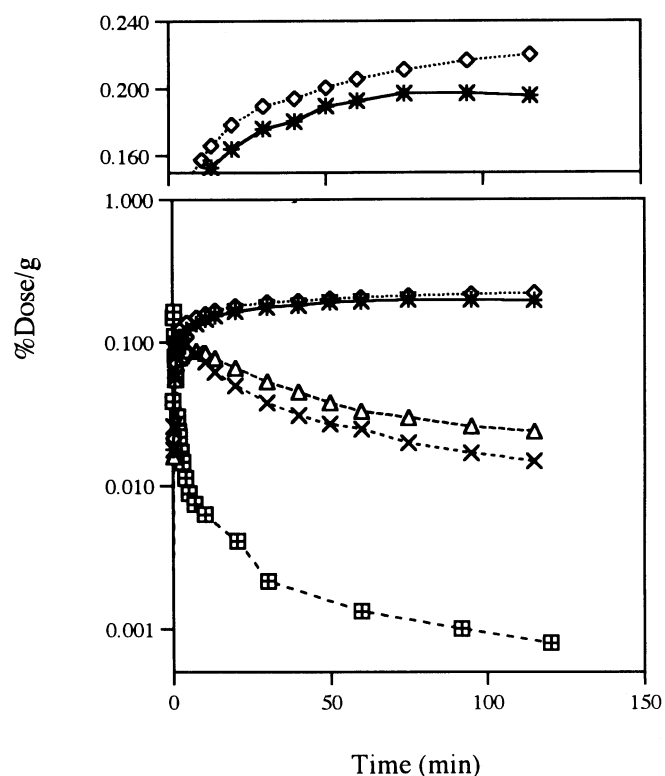


FIG. 6. Time-activity curves for average of left and right putamen (\*), left and right caudate (◇), cortex (Δ), cerebellum (X), and parent in plasma (□) of a rhesus monkey's brain after receiving 3.13 mCi of 2β-carbomethoxy-3β-(4-chlorophenyl)-8-(3-fluoropropyl)nortropine ( $^{18}\text{F}$ ]FPCT). Serial images were acquired for a total time of 125 min (i.e., 18 scans).

## RESULTS

### Radiolabeling

Fluorine-18 labeled FECNT was prepared following target bombardment by a two step reaction sequence that first involved the preparation of the radiolabeled precursor 1- $^{18}\text{F}$ ]fluoro-2-tosyloxyethane (5) in 68% yield, corrected for decay at EOB (Fig. 1). Alkylation of 1- $^{18}\text{F}$ ]fluoro-2-tosyloxyethane with 2β-carbomethoxy-3β-(4-chlorophenyl)nortropine in DMF at 135°C afforded  $^{18}\text{F}$ ]FECNT in 21% overall yield corrected for decay at EOB, in a synthesis time of 122 min including HPLC purification. Final purification of  $^{18}\text{F}$ ]FECNT by semi-preparative, reverse-phase HPLC column resulted in a product free from the precursor 2β-carbomethoxy-3β-(4-chlorophenyl)nortropine, with a chemical and radiochemical purity >99% and with a specific activity of 2 Ci/ $\mu\text{mole}$  (Fig. 2).

### In Vitro Binding in Human DAT Expressing Cells and Rat Brain Homogenates

The *in vitro* affinity of FECNT for DAT was determined by competition in DAT radioligand binding. The results for competition for  $^3\text{H}$ ]WIN 35428 binding in homogenates of murine kidney cells stably expressing the human DAT are shown in Table 1. The rank order of affinities was GBR 12909 > CIT >> FPCT > FECNT. FECNT had four and three times lower affinity than GBR 12909 and CIT, respectively, for the transfected human DAT. In

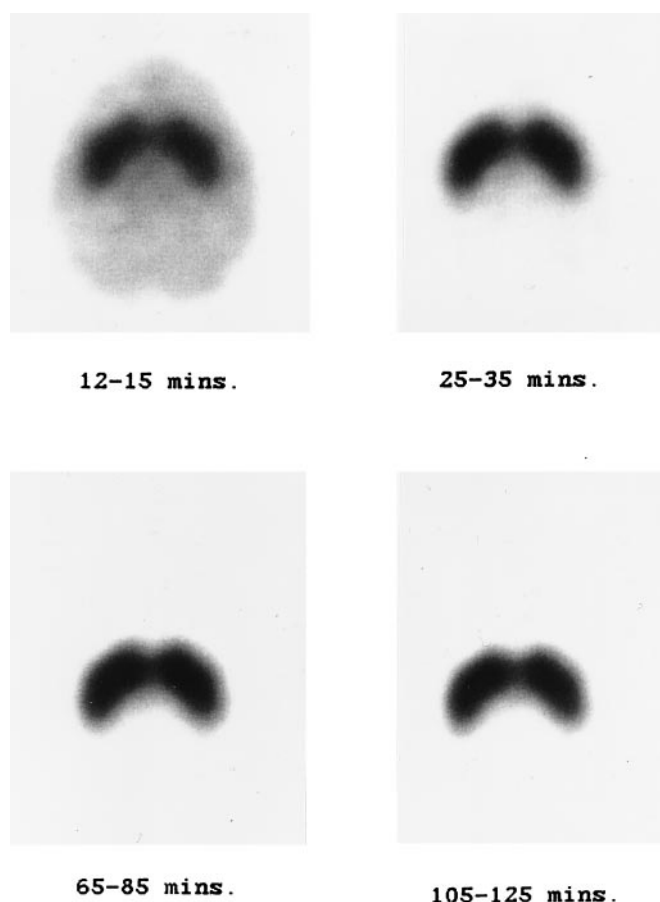


**FIG. 7.** Transaxial images for a single plane image following fluorine-18 labeled 2 $\beta$ -carbomethoxy-3 $\beta$ -(4-chlorophenyl)-8-(2-fluoroethyl)nortropine ([ $^{18}\text{F}$ ]FECNT) summed for 12–15 min, 25–35 min, 65–85 min, and 105–125 min in a male rhesus monkey.

comparison to FPCT, FECNT had 30% lower affinity for DAT binding to rat striatal homogenates. Competition binding site analyses also were used to evaluate the comparative affinity of FECNT for the hSERT and hNET labeled by [ $^3\text{H}$ ]citalopram and [ $^3\text{H}$ ]nisoxetine, respectively (Table 1). The affinity of FECNT for the human SERT and NET was 25- and 156-fold lower, respectively, than for DAT. A lower selectivity for FECNT for the DAT versus SERT was noted for [ $^3\text{H}$ ]citalopram binding to rat cortical homogenates (Table 1). These results indicate that FECNT exhibits low affinity for the human or rat NET selective affinity for DAT versus SERT and an affinity for the human and rat DAT comparable to FPCT.

### ***In Vitro* Autoradiography**

The binding of [ $^{18}\text{F}$ ]FECNT was localized to the caudate nucleus and putamen in coronal sections through the rhesus caudate and lenticulate (Fig. 3). Nonspecific binding of [ $^{18}\text{F}$ ]FECNT (in the presence of 10 nM GBR 12909) was less than 5% of total binding. The highest density of binding sites was localized to the head of the caudate putamen whereas that of the putamen was approximately 90% that of the caudate; globus pallidus binding of [ $^{18}\text{F}$ ]FECNT was approximately 20% that of the caudate. GBR 12909 (100 nM) inhibited the striatal binding of [ $^{18}\text{F}$ ]FECNT by 50%. The NE

selective reuptake inhibitor reboxetine (100 nM) decreased FECNT binding by 15% in the head of the caudate and putamen. The 5-HT selective reuptake inhibitor paroxetine (100 nM) exhibited negligible effects on [ $^{18}\text{F}$ ]FECNT binding in the caudate or putamen. The DAT inhibitor CIT exhibited a concentration-dependent inhibition of [ $^{18}\text{F}$ ]FECNT binding in the caudate and putamen with an estimated  $\text{IC}_{50}$  of 8 nM and 11 nM (Fig. 4). A concentration of 100 nM of CIT was associated with a maximal inhibition (85%) of [ $^{18}\text{F}$ ]FECNT binding in the head of the caudate and putamen. The *in vitro* pharmacology of [ $^{18}\text{F}$ ]FECNT binding was similar for autoradiograms of brain sections from a pigtailed (macaca nemestrina) macaque.

### ***In Vivo* Blocking Studies**

To determine the *in vivo* selectivity of FECNT for rat brain DAT, a series of blocking studies were performed in which unlabeled monoamine transporter specific blockers (5 mg/kg body weight of rat) were administered intravenously 15 min prior to the intravenous administration of [ $^{18}\text{F}$ ]FECNT. The rats were sacrificed 60 min after injection of [ $^{18}\text{F}$ ]FECNT and the striatum, cortex, prefrontal cortex, hypothalamus, and cerebellum were dissected and the uptake of radioactivity determined. The monoamine transporter blockers administered were GBR 12909 (DAT), paroxetine (SERT), and reboxetine (NET). The results of this study, shown in Table 2, clearly demonstrate that only GBR 12909 significantly blocked the uptake of [ $^{18}\text{F}$ ]FECNT in the DAT transporter rich striatum. Compared with the no blocker group, the SERT and NET blocking agents showed no effect on the regional brain uptake of [ $^{18}\text{F}$ ]FECNT.

### ***PET Nonhuman Primate Imaging***

The monkey brain regional distribution of radioactivity (without partial volume correction), expressed as percent dose per gram, after the intravenous administration of [ $^{18}\text{F}$ ]FECNT is shown in Figure 5. A high initial uptake of radioactivity in the brain occurred after injection of [ $^{18}\text{F}$ ]FECNT. The uptake percentage of FECNT in the cerebellum (CB) and cortex (CX) exhibited a maximum value of 0.09 %dose/g at 2.75 min and 0.065% dose/g, respectively, at 4.5 min postinjection. The caudate and putamen exhibited the highest uptake of brain radioactivity with prolonged retention. The putamen attained maximum (0.194 %dose/g) uptake at 75 min. The putamen-to-cerebellum and putamen-to-cortex ratios exhibited rapid and pronounced increases with marginal ratios of 12.7 at 115 min. Caudate radioactivity indicated a peak uptake of 0.2 %dose/g at 60 min and a caudate-to-cerebellum ratio of 12.3 at 115 min.

The uptake and retention of [ $^{18}\text{F}$ ]FECNT (Fig. 5) and [ $^{18}\text{F}$ ]FPCT (Fig. 6) were compared in the caudate and putamen in the same rhesus monkey. [ $^{18}\text{F}$ ]FECNT reached a decay-corrected peak uptake in the caudate and putamen at 60 and 75 min postinjection, respectively, whereas the decay-corrected uptake of [ $^{18}\text{F}$ ]FPCT continued to increase at 115 min postinjection. The parallel time activity curves for the caudate, putamen, cortex, and cerebellum following [ $^{18}\text{F}$ ]FECNT (Fig. 5) suggest that binding site equilibrium was attained. The summed images, collected from 12 min to 115 min following tracer injection, for a transverse plane through the basal ganglia, are shown in Figure 7. The caudate and putamen are the only brain regions visibly labeled by [ $^{18}\text{F}$ ]FECNT at 115 min.

The *in vivo* binding of [ $^{18}\text{F}$ ]FECNT to DAT in the putamen of two rhesus monkeys was demonstrated further by measuring the displacement of radioactivity induced by the administration of the



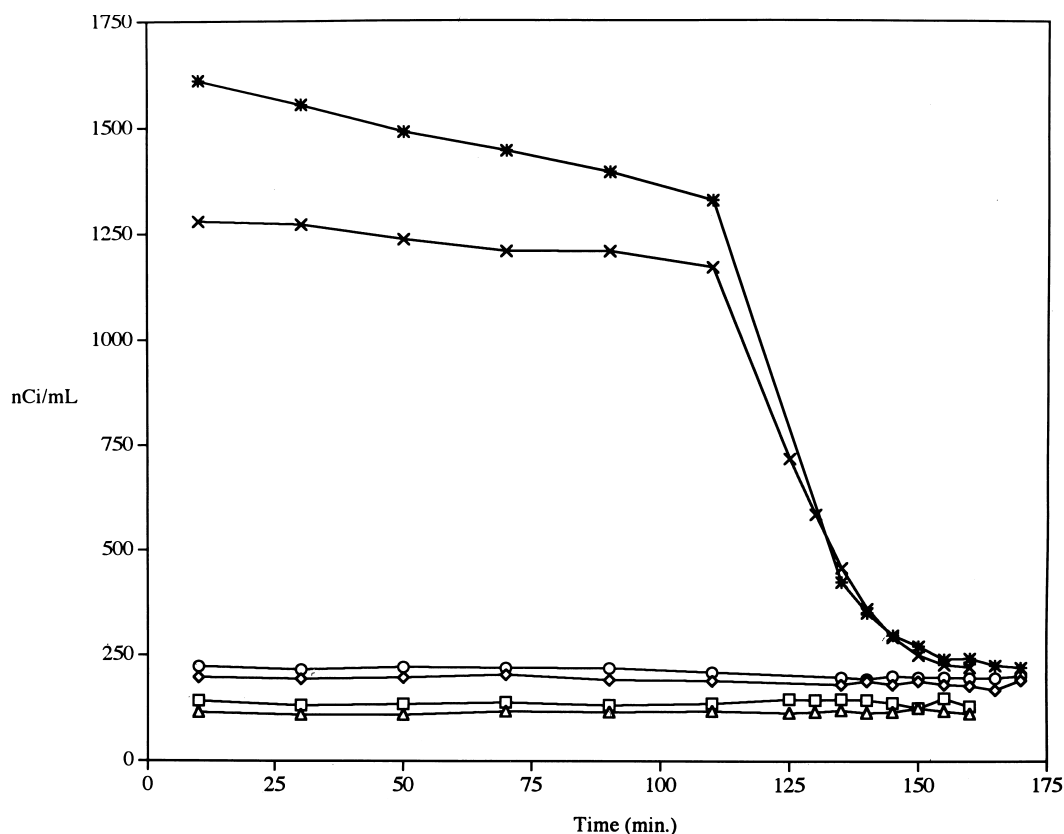


FIG. 8. Time-activity curves for average of left and right putamen (\*), left and right cortex (◇), and cerebellum (○) brain regions of a rhesus monkey after receiving 4.12 mCi of fluorine-18 labeled 2 $\beta$ -carbomethoxy-3 $\beta$ -(4-chlorophenyl)-8-(2-fluoroethyl)nortropine ( $^{18}\text{F}$ ]FECNT) and displacement by 0.9  $\mu\text{mole/kg}$  CIT administered 210 min after injection of  $^{18}\text{F}$ ]FECNT. Serial images were acquired from 90 to 260 min postinjection of  $^{18}\text{F}$ ]FECNT for a total time of 170 min (i.e., 14 scans). Time-activity curves for average of left and right putamen (x), average of left and right cortex (Δ), and cerebellum (□) brain regions of a rhesus monkey after receiving 2.12 mCi of  $^{18}\text{F}$ ]FECNT and displacement with 0.9  $\mu\text{mole/kg}$  CIT administered 210 min after injection of  $^{18}\text{F}$ ]FECNT. Serial images were acquired from 90 to 250 min after injection of  $^{18}\text{F}$ ]FECNT for a total time of 160 min (i.e., 14 scans).

DAT high affinity ligand CIT 210 min following injection of  $^{18}\text{F}$ ]FECNT. A 0.9  $\mu\text{mol/kg}$  dose of unlabeled CIT produced a rapid and large decrease in  $^{18}\text{F}$ ]FECNT binding to the putamen (Fig. 8). The average half-time of displacement was 10.2 min.

### Biotransformation of $^{18}\text{F}$ ]FECNT

Arterial plasma samples from rhesus monkeys ( $N = 4$ ) following femoral vein injection of  $^{18}\text{F}$ ]FECNT were analyzed for nonpolar, potentially brain permeable, metabolites by a solvent extraction and HPLC-UV method (2). The major radioactive component appearing in the initial arterial plasma samples was ether extractable, displayed a single peak (>98% pure) on both TLC and HPLC, and corresponded to unmetabolized authentic  $^{18}\text{F}$ ]FECNT. The fraction of plasma radioactivity corresponding to unmetabolized  $^{18}\text{F}$ ]FECNT rapidly decreased from 91% at 2 min to 33% at 15 min. The major radiolabeled metabolite found in arterial plasma was a polar nonextractable component, which increased to 94% of the plasma activity by 120 min. The arterial input function for  $^{18}\text{F}$ ]FECNT in the rhesus monkey ( $N = 4$ ) is shown in Figure 9. Following slow bolus (30 s) intravenous administration of  $^{18}\text{F}$ ]FECNT peak arterial plasma fluorine-18 radioactivity was attained at 2.4 min. The arterial plasma fraction corresponding to unmetabolized  $^{18}\text{F}$ ]FECNT had a half-life of 78 min following its administration.

Supernatants of rat striatal homogenates were similarly analyzed for metabolites of  $^{18}\text{F}$ ]FECNT 2 and 60 min following an intravenous injection of 1.0 mCi of  $^{18}\text{F}$ ]FECNT. Radioactivity in the supernatant was 81% and 80% of total at 2 and 60 min postinjection, respectively. The fluorine-18 radioactivity in the supernatant at 2 and 60 min postinjection was 70% and 54% extractable by ethyl ether, respectively. The ether-extracted radioactivity eluted as a single peak (99% pure) on HPLC and corresponded to unmetabolized, authentic FECNT. The radioactivity remaining in the supernatant after ether extraction was separated by HPLC and quantitated using a gamma-counter. At 2 and 60 min postinjection, 99% and 95% of the radioactivity in the supernatant, respectively, co-eluted with authentic FECNT.

### DISCUSSION

$^{18}\text{F}$ ]FECNT, a high affinity ligand for brain DAT, was radiofluorinated by a two-step synthesis using no-carrier added  $^{18}\text{F}$ ]fluoride (283 mCi  $\text{K}^{18}\text{F}$ ) and a commercially available precursor 1,2-ditosyloxyethane (Fig. 1). The synthesis is amenable to automation (13) and yielded 26.5 mCi of  $^{18}\text{F}$ ]FECNT at end of synthesis (EOS) with a specific activity of 2 Ci/ $\mu\text{mol}$ .

Comparison of *in vivo* imaging studies in the same rhesus monkey demonstrated that both  $^{18}\text{F}$ ]FECNT and  $^{18}\text{F}$ ]FPCNT showed high preferential uptake in the caudate and putamen with relatively low

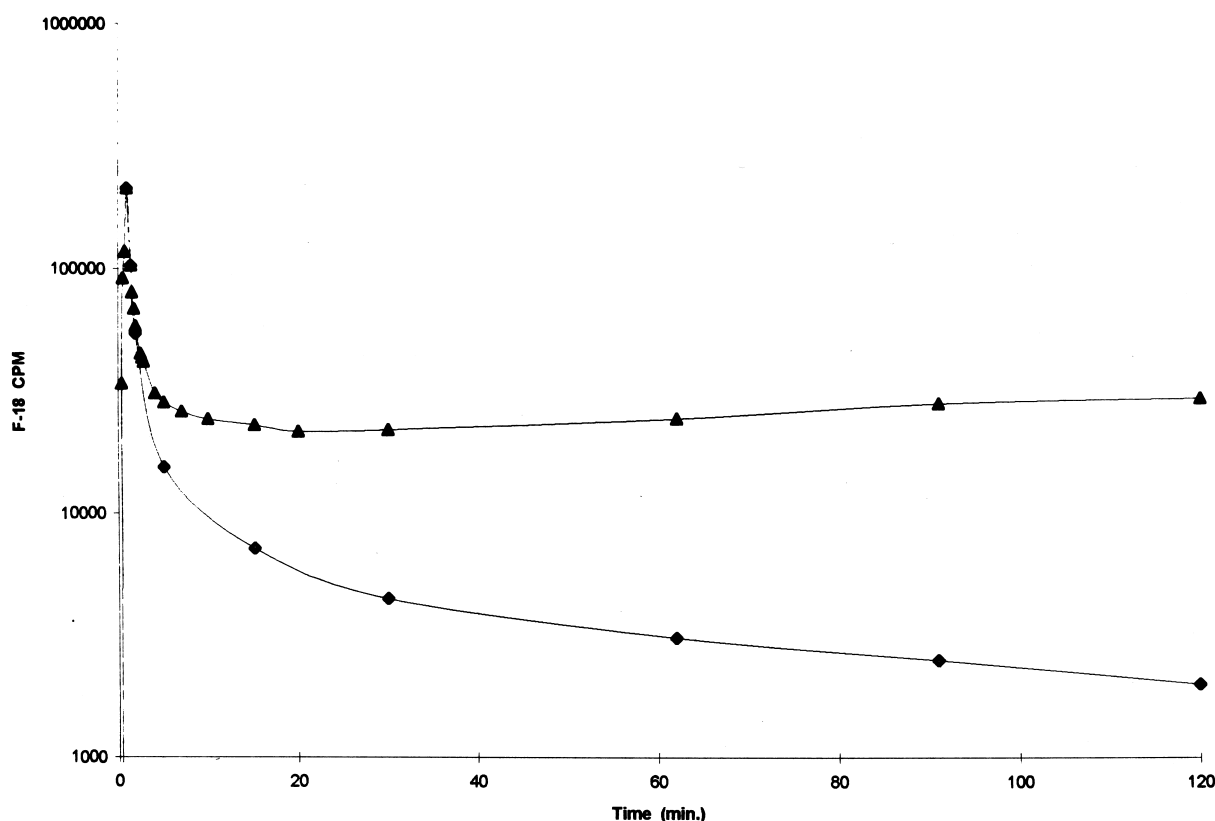


FIG. 9. Arterial input function for [ $^{18}\text{F}$ ] in a male rhesus monkey following administration of 5.88 mCi of fluorine-18 labeled 2 $\beta$ -carbomethoxy-3 $\beta$ -(4-chlorophenyl)-8-(2-fluoroethyl)nortropane ([ $^{18}\text{F}$ ]FECNT). Total arterial  $^{18}\text{F}$  plasma activity (▲) and arterial parent [ $^{18}\text{F}$ ]FECNT activity (◆).

uptake in the hypothalamus/midbrain, cerebral cortex, and cerebellum. The ratios of caudate- and putamen-to-cortex/cerebellum were 10.5-to-1 at 60 min, the time reached for transient equilibrium for [ $^{18}\text{F}$ ]FECNT. The specific-to-nonspecific binding ratios for [ $^{18}\text{F}$ ]FECNT reached at transient equilibrium are greater than the PET DAT ligands [ $^{11}\text{C}$ ]β-CIT-FE (16) and [ $^{18}\text{F}$ ]β-CIT-FP (23), which were 9 and 5, respectively. Binding of [ $^{18}\text{F}$ ]FECNT in the caudate nucleus and putamen reached a maximum at 60–75 min postinjection and declined at a rate of 8%/h. In contrast to [ $^{18}\text{F}$ ]FECNT, the caudate nucleus and putamen uptake of [ $^{18}\text{F}$ ]FPCT steadily increased over the 2-h collection of emission data and was still increasing 125 min postinjection. The ratios of caudate- and putamen-to-cortex/cerebellum were 12-to-1 at 125 min for [ $^{18}\text{F}$ ]FPCT. The higher striatal uptake and retention of [ $^{18}\text{F}$ ]FPCT relative to [ $^{18}\text{F}$ ]FECNT may be attributed, in part, to the 30% higher affinity of [ $^{18}\text{F}$ ]FPCT for the DAT (15). The 12-to-1 ratios of caudate- and putamen-to-cortex/cerebellum observed for both [ $^{18}\text{F}$ ]FECNT and [ $^{18}\text{F}$ ]FPCT at 125 min, despite the large difference in reversible binding, may be explained by the fact that [ $^{18}\text{F}$ ]FPCT is more lipophilic than [ $^{18}\text{F}$ ]FECNT, which results in a slower clearance of [ $^{18}\text{F}$ ]FPCT from the cortex/cerebellum than [ $^{18}\text{F}$ ]FECNT. The observation of a longer retention time for [ $^{18}\text{F}$ ]FPCT (31 min) (15) on the same column and with the same solvent during HPLC purification in comparison to that of [ $^{18}\text{F}$ ]FECNT (21 min) is consistent with a higher degree of lipophilicity for [ $^{18}\text{F}$ ]FPCT.

*In vitro* displacement studies with murine kidney cells transfected with cDNAs for human dopamine, serotonin, and norepinephrine transporters and with rat brain tissue demonstrated that FECNT

competed with high affinity for [ $^3\text{H}$ ]WIN 35428 binding to the DAT. The affinity of FECNT for [ $^3\text{H}$ ]WIN 35428 binding in murine kidney cells stably expressing the human DAT and in rat striatum was approximately one third that of GBR 12909 and CIT. The high DAT selectivity of FECNT was demonstrated in *in vitro* competitive binding experiments in transfected murine kidney cells with the labeled serotonin and norepinephrine transporter ligands [ $^3\text{H}$ ]citalopram and [ $^3\text{H}$ ]nisoxetine. Compared with DAT, FECNT exhibited 25-fold and 152-fold lower affinity for the serotonin transporter and the norepinephrine transporter, respectively. *In vitro* autoradiography confirmed that [ $^{18}\text{F}$ ]FECNT binding in the rhesus caudate and putamen reflected a selective labeling of DAT.

An *in vivo* PET study of [ $^{18}\text{F}$ ]FECNT displacement by CIT was performed to determine whether putamen radioactivity reflected [ $^{18}\text{F}$ ]FECNT binding to DAT. A high dose (0.9  $\mu\text{mole/kg}$ ) of CIT resulted in a rapid and dramatic reduction of radioactivity in the putamen (Fig. 8). Prior to CIT administration, [ $^{18}\text{F}$ ]FECNT putamen binding reached an equilibrium state within 90 min and was declining at an average rate of 0.13%/min. Following CIT administration, [ $^{18}\text{F}$ ]FECNT putamen binding exhibited an average wash-out rate of 3.5%/min. Forty minutes following the administration of CIT, 78% of the [ $^{18}\text{F}$ ]FECNT radioactivity had been displaced. CIT is a potent antagonist of both DAT and SERT (2). The low uptake of [ $^{18}\text{F}$ ]FECNT in the hypothalamus/thalamus brain regions of high SERT density and negligible displacement of radioactivity from the cortex and cerebellum by CIT further indicate that [ $^{18}\text{F}$ ]FECNT binding reflects DAT labeling.

Analysis of ether extracts of monkey arterial plasma samples using HPLC separation and gamma-counter detection showed the

rapid appearance of one major polar (non-ether extractable) metabolite of [<sup>18</sup>F]FECNT. The abundance as a percent of total plasma activity increased from 9% at 2 min to 94% at 120 min postinjection. The identity of the polar metabolite was not elucidated due to its improbable brain permeability. The remaining fraction of radioactivity in the arterial plasma was ether extractable and identified as unmetabolized [<sup>18</sup>F]FECNT. Thus, there was no detectable formation of lipophilic radiolabeled metabolites capable of entering the brain. The absence of labeled lipophilic metabolites in the arterial plasma that could reenter the brain permits the metabolism uncorrected calculation of the [<sup>18</sup>F]FECNT input function and subsequent quantification of binding sites by tracer kinetic modeling.

In conclusion, *in vivo* imaging studies demonstrated that [<sup>18</sup>F]FECNT, relative to [<sup>11</sup>C]WIN 35,428, [<sup>11</sup>C]CIT/RTI-55, and [<sup>18</sup>F]FPCT, has more attractive kinetic characteristics as a DAT PET ligand by achieving peak striatal uptake in less than 2 h and higher caudate/putamen-to-cerebellar ratios. Thus, [<sup>18</sup>F]FECNT represents a unique selective DAT transporter ligand labeled with the PET radionuclide fluorine-18. Its 110 min half-life allows time for incorporation into the tracer molecule, purification of the final product, and accurate measurement by PET of the kinetic constants of compartmental models used to estimate regional brain densities of DAT. In addition, the 110 min half-life enables its geographic distribution to sites with newly developed coincidence high energy gamma cameras and permits widespread patient and research use. These results suggest that [<sup>18</sup>F]FECNT is a promising new tool for *in vivo* mapping of brain DAT in humans by PET.

*This research was sponsored by the Office of Health and Environmental Research, U.S. Department of Energy under Grant No. DE-FG05-93ER61737, and the National Institute of Mental Health Drug Screening Program. The authors thank Carolyn K. Malcolm for assistance in preparing the manuscript, and Delicia Votaw, Teresa Abak, and Elizabeth Smith for assistance in the data collection and analysis.*

## References

- Aquilonius S. M., Bergstrom K., Eckernas S. A., Hartvig P., Leenders K. L., Lundquist H., Antoni G., Gee A., Rimland A., Uhlin J. and Langstrom B. (1987) *In vivo* evaluation of striatal dopamine reuptake sites using 11C-nomifensine and positron emission tomography. *Acta Neurol. Scand.* **76**, 283–287.
- Baldwin R. M., Zea-Ponce Y., Zoghbi S., Laurelle M., Al-Tikriti M., Sysbirska E., Malison R. T., Neumeyer J. L., Milius R. A., Wang S., Stabin M., Smith E., Charney D. S., Hoffer P. B. and Innis R. B. (1993) Evaluation of the monoamine uptake site ligand ([<sup>123</sup>I]β-CIT) in non-human primates: Pharmacokinetics, biodistribution and SPECT brain imaging co-registered with MRI. *Nucl. Med. Biol.* **20**, 597–606.
- Bernheimer H., Birkmayer W. and Hornykiewicz O. (1973) Brain dopamine and the syndromes of Parkinson and Huntington: Clinical, morphological and neurochemical correlations. *J. Neurol. Sci.* **20**, 415–455.
- Billings J., Kung M. P., Chumpradit S., Mozley D., Alavi A. and Kung H. F. (1991) Characterization of radio-iodinated TISCH: A high affinity and selective ligand for mapping CNS dopamine D-1 receptor. *J. Neurochem.* **58**, 227–236.
- Block D., Coenen H. H. and Stocklin G. (1987) The N.C.A. nucleophilic <sup>18</sup>F-fluorination of 1,N-disubstituted alkanes as fluoroalkylation agents. *J. Labelled Compd. Radiopharm.* **24**, 1029–1042.
- Carroll F. I., Lewin A. H., Boja J. W. and Kuhar M. J. (1992) Cocaine receptor: Biochemical characterization and structure-activity relationships of cocaine analogues at the dopamine transporter. *J. Med. Chem.* **35**, 969–981.
- Chaly T., Dhawan V., Kazumata K., Antonini A., Margoulef C., Dahl R., Belakhef A., Margoulef D., Yee A., Wang S., Tamagnan G., Neumeyer J. L. and Eidelberg D. (1996) Radiosynthesis of [18F]N-3-fluoropropyl-2-β-carbomethoxy-3-β-(4-iodophenyl) nortropine and the first human study with positron emission tomography. *Nucl. Med. Biol.* **23**, 999–1004.
- Dannals R. F., Neumeyer J. L., Milius R. A., Ravert H. T., Wilson A. A. and Wagner H. N. Jr. (1993) Synthesis of a radiotracer for studying dopamine uptake site *in vivo* using PET: 2β-Carbomethoxy-3β-(P-fluorophenyl)-[N-<sup>11</sup>C-methyl]tropine ([<sup>11</sup>C]CFT or [<sup>11</sup>C-WIN 35,428]). *J. Labelled Compd. Radiopharm.* **33**, 147–152.
- Ding Y., Fowler J., Volkow N., Logan J., Gatley S. and Sugano Y. (1995) Carbon-11-d-threo-methylphenidate binding to dopamine transporter in baboon brain. *J. Nucl. Med.* **36**, 2298–2305.
- Fowler J. S., Volkow N. D., Wolf A. P., Dewey S. L., Schlyer D. J., Macgregor R. R., Hitzemann R., Logan J., Bendriem B. and Gatley S. J. (1989) Mapping cocaine binding sites in human and baboon brain *in vivo*. *Synapse* **4**, 371–377.
- Frost J. J., Rosier A. J., Reich S. G., Smith J. S., Ehlers M. D., Snyder S. H., Ravert H. T. and Dannals R. F. (1993) Positron emission tomographic imaging of the dopamine transporter with <sup>11</sup>C-WIN 35,428 reveals marked declines in mild Parkinson's disease. *Ann. Neurol.* **34**, 423–431.
- Giros B., Jaber M., Jones S. R., Wightman R. M. and Caron M. G. (1996) Hyper-locomotion and indifference to cocaine and amphetamine in mice lacking the dopamine transporter. *Nature* **379**, 606–612.
- Goodman M. M. (1991) Automated synthesis of radiotracers for positron emission tomography applications. In: *Clinical Positron Emission Tomography (PET)* (Edited by Hubner K. F., Buonocore E., Colmann J. and Kabalka G. W.), pp. 110–122. Mosby-Year Book, Inc., St. Louis, MO.
- Goodman M. M., Kabalka G. W., Kung M. P., Kung H. F. and Meyer M. A. (1994) Synthesis of [<sup>18</sup>F]-N-3-fluoropropyl-2β-carbomethoxy-3β-4-chlorophenyl)tropane: A high affinity neurologist to map dopamine uptake sites by PET. *J. Labelled Compd. Radiopharm.* **34**, 488–490.
- Goodman M. M., Keil R., Shoup T. M., Eshima D., Eshima L., Kilts C., Votaw J., Camp V. M., Votaw D., Smith E., Kung M. P., Malveaux E., Watts R., Huerkamp M., Garcia E. and Hoffman J. M. (1997) Fluorine-18 labeled 2β-carbomethoxy-3β-(4-chlorophenyl)-8-(3-fluoropropyl)nortropine (FPCT): A PET radiotracer for imaging dopamine transporters. *J. Nucl. Med.* **38**, 119–126.
- Halldin C., Farde L., Lundkvist C., Ginovart N., Nakashima Y., Karlson P. and Swahn C. (1996) [<sup>11</sup>C]β-CIT-FE, a radioligand for quantitation of the dopamine transporter in the living brain using positron emission tomography. *Synapse* **22**, 386–390.
- Kaufman M. J. and Madras B. K. (1991) Severe depletion of cocaine recognition sites associated with the dopamine transporter in Parkinson's diseased striatum. *Synapse* **49**, 43–49.
- Kilbourn R. and Haka M. S. (1988) Synthesis of [18F]GBR 13119: A pre-synaptic dopamine uptake antagonist. *Appl. Radiat. Isot.* **39**, 279–282.
- Kilbourn M. R. (1988) *In vivo* binding of [18F]GBR 13119 to the brain dopamine uptake system. *Life Sci.* **42**, 1347–1353.
- Kilbourn M. R., Carey J. E., Koeppe R. A., Haka M. S., Hutchins G. A., Sherman P. S. and Kuhl D. E. (1989) Biodistribution, dosimetry, metabolism and monkey PET studies of [18F]GBR 13119. Imaging the dopamine uptake system *in vivo*. *Nucl. Med. Biol.* **16**, 569–576.
- Logan J., Fowler J. S., Volkow N. D., Wolf A. P., Dewey S. L., Schlyer D. J., Macgregor R. R., Hitzemann R., Bendriem B., Gatley S. J. and Christman D. R. (1990) Graphical analysis of reversible radioligand binding from time-activity measurements applied to measurements applied to [N-<sup>11</sup>C-methyl]-(-)-cocaine PET studies in human subjects. *J. Cereb. Blood Flow Metab.* **5**, 740–747.
- Lundkvist C., Halldin C., Swahn C. G., Hall H., Karlson P., Nakashima Y., Wang S., Milius R. A., Neumeyer J. L. and Farde L. (1995) [O-Methyl-<sup>11</sup>C]β-CIT-FP, a potential radioligand for quantitation of the dopamine transporter: Preparation, autoradiography, metabolite studies, and positron emission tomography examinations. *Nucl. Med. Biol.* **22**, 905–913.
- Lundkvist C., Halldin C., Ginovart N., Swahn C. and Farde L. (1997) [<sup>18</sup>F]β-CIT-FP, for quantitation of the dopamine transporter. *Nucl. Med. Biol.* **24**, 621–627.
- Meltzer P. C., Liang A. Y., Brownell A. L., Elmaleh D. R. and Madras B. K. (1993) Substituted 3-phenyltropane analogs of cocaine: Synthesis, inhibition of binding at cocaine recognition sites, and positron emission tomography imaging. *J. Med. Chem.* **36**, 855–862.
- Muller L., Halldin C., Farde L., Karlson P., Hall H., Swahn C. G., Neumeyer J. L., Wang S. and Milius R. A. (1993) [<sup>11</sup>C]β-CIT, a cocaine

- analogue. Preparation, autoradiography and preliminary PET investigations. *Nucl. Med. Biol.* **20**, 249–255.
26. Niznik H. B., Fogel E. F., Fassos E. F. and Seeman P. (1991) The dopamine transporter is absent in Parkinson's putamen and reduced in the caudate nucleus. *J. Neurochem.* **56**, 192–198.
27. Volkow N. D., Wang G. J., Fischman M. W., Foltin R. W., Fowler J. S., Abumrad N. N., Vitkun S., Logan J., Gatley S. J., Pappas N., Hitzemann R. and Shea C. E. (1997) Relationship between subjective effects of cocaine and dopamine transporter occupancy. *Nature* **386**, 827–830.
28. Wilson A. A., DaSilva J. N. and Houle S. (1996) In vivo evaluation of [11C]- and [18F]-labelled cocaine analogues as potential dopamine transporter ligands for positron emission tomography. *Nucl. Med. Biol.* **23**, 141–146.